Redox Biology 58 (2022) 102542

Contents lists available at ScienceDirect

Redox Biology

journal homepage: www.elsevier.com/locate/redox

Sigma-1 receptor agonist PRE-084 confers protection against TAR DNA-binding protein-43 toxicity through NRF2 signalling

Christelle Lasbleiz [a,b,1], Amandine Peyrel [a,1], Pauline Tarot [a,1], Jérôme Sarniguet [a], Lucie Crouzier [a], Nicolas Cubedo [a], Benjamin Delprat [a], Mireille Rossel [a,b], Tangui Maurice [a], Jean-Charles Liévens [a,*]

[a] MMDN, Univ Montpellier, EPHE, INSERM, Montpellier, France
[b] EPHE, PSL, Paris, France

A B S T R A C T

Amyotrophic lateral sclerosis (ALS) is a neurodegenerative disease affecting upper and lower motor neurons. As a consequence, ALS patients display a locomotor disorder related to muscle weakness and progressive paralysis. Pathological mechanisms that participate in ALS involve deficient unfolded protein response, mitochondrial dysfunction and oxidative stress, among others. Finding a therapeutic target to break the vicious circle is particularly challenging. Sigma-1 receptor (S1R) is an endoplasmic reticulum (ER) chaperone that may be one of those targets. We here address and decipher the efficiency of S1R activation on a key ALS gene, TDP43, in zebrafish vertebrate model. While expression of mutant TDP43 ($TDP43^{G348C}$) led to locomotor defects, treatment with the reference S1R agonist PRE-084 rescued motor performances in a zebrafish model. Treatment with the agonist ameliorated maximal mitochondrial respiration in the TDP43 context. We observed that $TDP43^{G348C}$ exacerbated ER stress induced by tunicamycin, resulting in increased levels of ER stress chaperone BiP and pro-apoptotic factor CHOP. Importantly, PRE-084 treatment in the same condition further heightened BiP levels but also EIF2α/ATF4 and NRF2 signalling cascades, both known to promote antioxidant protection during ER stress. Moreover, we showed that increasing *NRF2* levels directly or by sulforaphane treatment rescued locomotor defects of $TDP43^{G348C}$ zebrafish. For the first time, we here provide the proof of concept that PRE-084 prevents mutant TDP43 toxicity by boosting ER stress response and antioxidant cascade through NRF2 signalling.

1. Introduction

Amyotrophic lateral sclerosis (ALS) is a very disabling disorder characterized by muscle weakness and progressive paralysis. The disease is due to a degeneration of motor neurons in the spinal cord, brain stem and motor cerebral cortex. Ultimately, the disease rapidly evolves with respiratory distress and death within 5 years after the first motor symptoms in most cases. Currently, there is no cure for ALS and no effective treatment to halt or reverse the progression of the disease. The only available treatments with Riluzole and Edaravone have limited benefits [1,2].

ALS patients are divided into sporadic cases with no family history, accounting 90% of the total cases, and those with a clear genetic inheritance. ALS results from a complex interaction between both genetic and environmental factors. Advances in the understanding of ALS pathogenesis come from the identification of genes linked to ALS. Familial and sporadic cases are associated with mutations in genes encoding the *copper/zinc superoxide dismutase 1* (*SOD1*), *TAR DNA-binding protein of* 43 kDa (*TDP43*), *fused in sarcoma* (*FUS*) or the chromosome 9 open reading frame 72 (C9orf72) proteins, among others [3,4]. Of importance, TDP43 is ubiquitously expressed and localizes predominantly in the nucleus. However, it has been found that in the majority of ALS patients TDP43 abnormally accumulates in the cytoplasm and forms aggregates, suggesting that deregulation and mislocalization of wild-type TDP43 mediates both sporadic and familial ALS [5]. TDP43 is also found mislocalized in 45% of patients with frontotemporal lobar degeneration (FTLD). TDP43 plays a critical role in several steps of mRNA metabolism by regulating transcription, mRNA transport and stabilization into the cytoplasm, translation and microRNA processing [6]. TDP43 dysregulation leads to many cellular abnormalities including abnormal accumulation of unfolded protein, excitotoxicity, nucleocytoplasmic transport defects, mitochondrial dysfunction and oxidative damage. Finding a therapeutic target to alleviate all those defects is particularly challenging.

The sigma-1 receptor (S1R) is considered to promote cell survival in living systems. S1R is a cellular chaperone, still named receptor, as it can

* Corresponding author. University of Montpellier, INSERM, UM1198, CC 105, place Eugène Bataillon, F-34095, Montpellier, cedex 5, France.
E-mail address: jean-charles.lievens@umontpellier.fr (J.-C. Liévens).
[1] These authors contributed equally to this work.

https://doi.org/10.1016/j.redox.2022.102542
Received 20 July 2022; Received in revised form 8 November 2022; Accepted 14 November 2022
Available online 17 November 2022

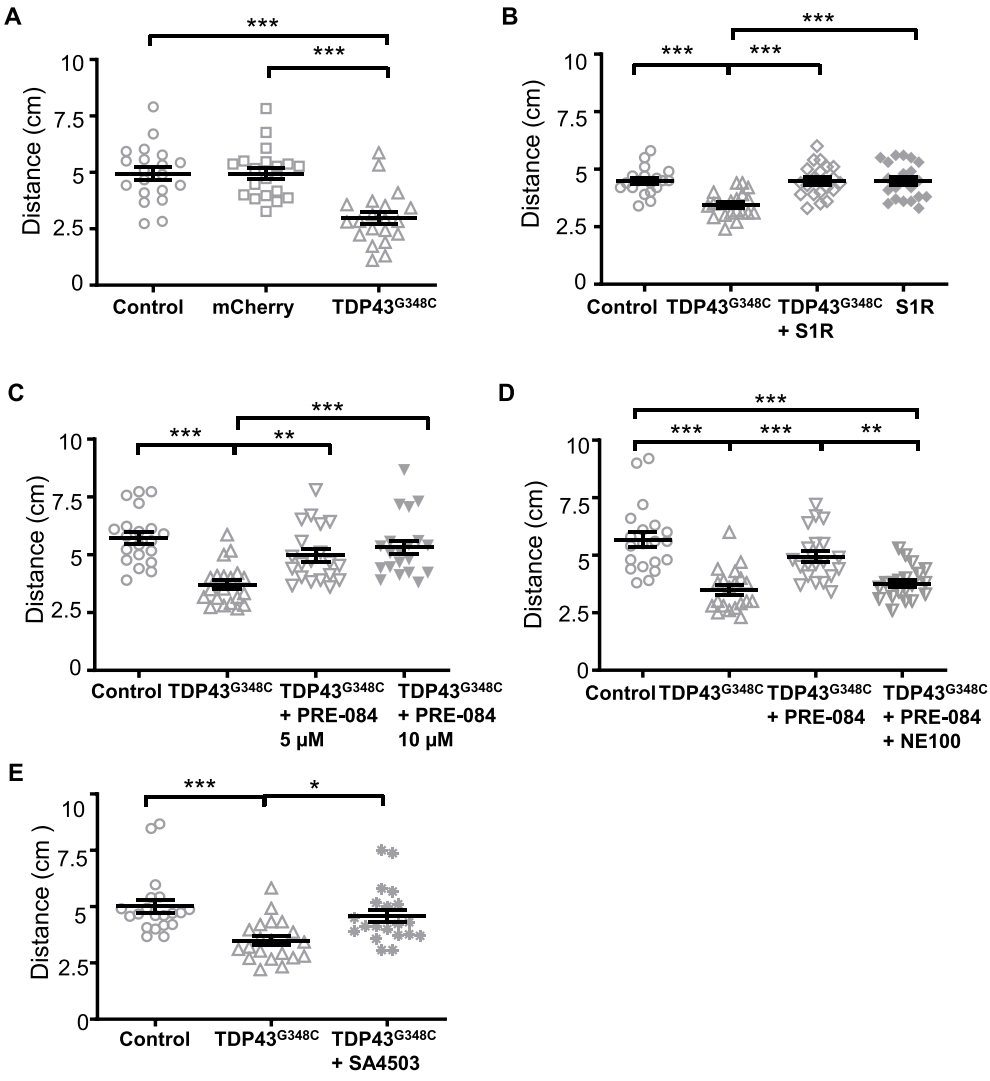

Fig. 1. S1R activation rescued touch-escape response of TDP43^{G348C}-expressing zebrafish larvae. (**A**) Touch-escape response of control larvae or larvae expressing mCherry alone or with TDP43^{G348C}. Swimming distance in 5 s was measured after tactile stimulation of 5 days post-fertilization (dpf) larvae. (**B**) Touch-escape response of control larvae or larvae expressing TDP43^{G348C}, TDP43^{G348C} + S1R or S1R alone. (**C**) Touch-escape response of control larvae, larvae expressing TDP43^{G348C} alone or treated with 5 or 10 µM of PRE-084. (**D**) Touch-escape response of control larvae or larvae expressing TDP43^{G348C} alone, treated with PRE-084 (5 µM) or treated with PRE-084 and NE-100 (5 µM each). (**E**) Touch-escape response of control, TDP43^{G348C} larvae treated or not with SA4503 (5 µM). In all figures data from 20 were averaged and presented as mean ± SEM. Statistical analysis was performed using ANOVA followed by Tukey's test (*$p < 0.05$; **$p < 0.01$; ***$p < 0.001$).

be activated/inactivated by small molecules, thus considered as S1R agonists or antagonists [7]. S1R is mostly located in the endoplasmic reticulum (ER), and more particularly at the mitochondria-associated ER membrane, where it modulates the inositol triphosphate (IP3) receptor type 3 to ensure proper Ca^{2+} signalling from the ER into mitochondria [8–11]. In case of accumulation of misfolded proteins, S1R can participate to the unfolded protein response, by acting on the inositol-requiring enzyme 1 (IRE1)/X-box binding protein 1 (XBP1) or activating transcription factor 4 (ATF4) pathways [12–14]. This leads to the subsequent expression of antioxidant proteins and chaperone proteins. Very interestingly, it has been proposed that during oxidative stress conditions S1R may also enhance nuclear production of antioxidant proteins by enhancing nuclear factor erythroid-2 related factor 2 (NRF2) signalling [15–17]. Moreover, upon over-expression or stimulation, S1R can translocate at the plasma membrane to modulate ion channels, receptors and kinases [12,18] or at the nuclear envelope to regulate nucleocytoplasmic trafficking and gene transcription [19,20].

In the last decade, S1R has been the focus of many studies on ALS. Not only, mutations in S1R were found to be the cause of juvenile cases of ALS [21,22], but also S1R knock-down exacerbated ALS-linked mutant SOD1 pathology in mouse models [22,23]. Of importance, S1R is a druggable target and its activation by agonists alleviated deficits of mutant SOD1 murine models [24–27]. Since mutations in SOD1 are linked to 15–20% of familial cases, observations from mice expressing this mutant protein do not allow extrapolating to the rest of ALS conditions. Further analyses are required to provide evidence that S1R is a valuable target to prevent ALS pathology. Of interest genetic approaches in *Drosophila* showed that overexpression of human S1R rescued locomotor defects of ALS flies expressing either TDP43 or the C9ORF72 mutation [20,28]. In the present study, we provide the proof of concept that S1R activators are efficient therapeutic strategies to reduce TDP43-induced damages in a vertebrate model.

2. Materials and methods

2.1. Drugs

2-(4-Morpholinethyl)-1-phenylcyclohexanecarboxylate hydrochloride (PRE-084), 1-(3,4-Dimethoxyphenethyl)-4-(3-phenylpropyl)piperazine) dihydrochloride (SA4503), 1-isothiocyanato-4-methylsulfinylbutane (sulforaphane) and tunicamycin were from Sigma-Aldrich (Saint-Quentin-Fallavier, France). 4-Methoxy-3-*N*,*N*-dipropylbenzeneethanamine (NE-100) was purchased from Tocris (Tebu-Bio, Le-Perray-En-Yvelines, France). PRE-084, SA4503 and NE-100 were solubilized in water and tunicamycin (10 mg/ml) and sulforaphane (4 mg/ml) in pure DMSO (Sigma-Aldrich).

2.2. Zebrafish generation and housing

All experiments were performed with zebrafish (*Danio rerio*, wild-

Table 1
Primers used for RT-qPCR.

	Forward primer	Reverse primer
ATF6	5′-CTGTGGTGAAACCTCCACCT-3′	5′-CATGGTGACCACAGGAGATG-3′
ATF4α	5′-CCGGGAATCATGGCAGTGTA-3′	5′GAGAAGCTGCGGTATTTGCG-3′
ATF4b	5′-TGACCCTCTGCGGTCAATTC-3′	5′-ACGAATGATCTTCACCACTGTCT-3′
BiP	5′-AAGAGGCCGAAGAGAAGGAC-3′	5′-AGCAGCAGAGCCTCGAAATA-3′
CHOP	5′-AAGGAAAGTGCAGGAGCTGA-3′	5′-TGTGAGCCTTCTCCGTCTTT-3′
EIF2α	5′-CCAAAGATGAGCAGCTGGAGA-3′	5′-ATCCGACACAGCCTGCTTAAA-3′
EF1α	5′-TTCTGTTACCTGGCAAAGGG-3′	5′-TTCAGTTTGTCCACACCCA-3′
GCLC	5′-ATCCGCCATAGGAGGGGTGA-3′	5′-TAGATGTGATCCGGCTTGGCA-3′
GCLM	5′-CTGAAGCTTCACACGGGGAAT-3′	5′-CGCTCAATGTGCCTTGAATGC-3′
IRE1	5′-TGACGTGGTGGAAGTTGGTA-3′	5′-ACGGATCACATTGGGATGTT-3′
KEAP1α	5′-TCTGCTGCATTTGCCCTTCA-3′	5′-GTAACCGTGACCCCTCATGGA-3′
KEAP1b	5′-GTTCCTGCTGGTGATGAGCG-3′	5′-CGTCACCTCCGCCTTACACT-3′
NRF2α	5′-CTCCCAGACTTGCAGCAGT-3′	5′-CACTTCTGTTTGAGCCGAGC-3′
NRF2b	5′-GTCGCTGCCAGATTTACAGTATT-3′	5′-GGGCAGGCATGGTAAAGAGT-3′
PGD	5′-ATGCAGCTGATCTGTGAGGC-3′	5′-AGGAAGGAGTCCAGCTCTGTC-3′
PRDX6	5′-GAAACAGTCATGCCTGGGATA-3′	5′-GACCAACTACAAACACGCAG-3′
Unspliced *XBP1*	5′-GGGTTGGATACCTTGGAAA-3′	5′-AGGGCCAGGGCTGTGAGTA-3′
Spliced *XBP1*	5′-TGTTGCGAGACAAGACGA-3′	5′-CCTGCACCTGCTGCGGACT-3′

type “Tuebingen” strain) in accordance with the 2010/63/EU Directive and the ARRIVE guidelines. Zebrafish were maintained in an automated fish tank system (ZebTEC, Tecniplast) at 28 °C, pH 7, a conductivity of 500 μS/cm and with a 14 h:10 h light:dark cycle. They were fed with pellets of Gemma Micro 500 (soluble hydrolyzed marine proteins, highly unsaturated fatty acids, phospholipids and alga) every day (Skretting France, Fontaine les Vervins, France). To generate transgenic zebrafish expressing human S1R, the cDNA encoding human *wild-type S1R* was inserted upstream of the *β-actin* promoter (UMS Amagen, Gif-Sur-Yvette, France). The transgene was injected into one cell zebrafish embryo (wild-type “Tuebingen” strain) and genome inserted by using the Tol2 transposable element (UMS Amagen) [29]. For selection of S1R + zebrafish, the YFP sequence was inserted upstream of the *cardiac actin* promoter. For experiments, heterozygous transgenic S1R zebrafish were intercrossed to wild-type (Tuebingen) zebrafish line to generate wild-type and heterozygous transgenic S1R zebrafish with fluorescent heart. The breeding diagram is shown in Supp. Fig. 1B. Zebrafish larvae with or without YFP fluorescent heart were separated using a fluorescent binocular loupe (Olympus MVX10).

2.3. mRNA injection

Transcripts encoding human mutant TDP43 ($TDP43^{G348C}$) were generated from the previously reported plasmid pCS2+$TDP43^{G348C}$ (generous gift from Dr. Pierre Drapeau, University of Montréal). The G348C mutation has been previously used as ALS models in worms, *Drosophila*, zebrafish and mouse [30]. The PCS2+ plasmid containing mCherry coding sequence (generous gift from Dr. Georges Lutfalla, LPHI, Montpellier) was used to check the correct injection of embryos. The pCS2+ NRF2 plasmid (generous gift from Pr. Masayuki Yamamoto, University of Tsukuba, Japan) [31] was used for testing direct overexpression of *NRF2*. $TDP43^{G348C}$, *NRF2*, and *mCherry* mRNAs were transcribed from Not1-linearized pCS2+ plasmid using the SP6 polymerase with the mMESSAGE Machine kit (Invitrogen-Thermo Fisher Scientific, Courtaboeuf, France) and purified according to the manufacturer’s instructions. Transcripts were microinjected into 1- to 2-cell--stage embryos according to standard protocols. Optimal mRNA concentrations have been determined using a range of dilutions. A volume of 1 nl was injected in each embryo at the one cell stage with the following concentrations depending of experimental conditions: for *mCherry* alone 140 ng/μl; for $TDP43^{G348C}$ + *mCherry* 40 and 100 ng/μl, respectively; for $TDP43^{G348C}$ + *NRF2* + *mCherry* 40, 25 and 100 ng/μl, respectively. At day 1, zebrafish larvae with a suitable expression level of red fluorescent mCherry were sorted out using a fluorescent binocular loupe (Olympus MVX10).

2.4. Quantitative real-time PCR (qPCR)

Total RNA was extracted from whole zebrafish larvae at 5 days post-fertilization (dpf) (n = 8–10 larvae/tube) using the NucleoSpin RNA kit (Macherey Nagel, Düren, Germany), following the manufacturer’s instructions. RNAs concentration and quality were evaluated using a NanoDrop One (Thermofisher Scientific, Les Ulis, France). Reverse transcription was performed using M-MLV Reverse Transcriptase (Promega, Charbonnières-les-Bains, France) following the manufacturer’s instructions. Reaction plates were prepared with diluted cDNAs and Sybr No-Rox Mix (Sensifast, Bioline, Ozyme, Saint-Cyr-L’Ecole, France) by an Echo 525 acoustic liquid handler (Labcyte, California, USA) and RT-qPCR experiments were performed by using a LightCycler 480 (Roche, Boulogne-Billancourt, France). The list of sequence for primers is summarized Table 1. RT-qPCRs were conducted for 45 cycles (10 s at 95 °C, 10 s at 60 °C, and 10 s at 72 °C) on LightCycler 480 system (Roche). Fold changes of gene expression were analyzed using the 2-ΔΔCp method [32]. Specific primers for amplifications of UPR genes were used (Table 1) and expression levels were normalized to the house-keeping gene *ef1α* (*ETS-related transcription factor*).

2.5. Western blot analysis

Whole larvae (n = 6) were homogenized in 80 μl RIPA lysis buffer (50 mM Tris-HCl, pH 8, 150 mM NaCl, 0.5% sodium deoxycholate, 0.1% sodium dodecyl sulfate, 1% Igepal CA-630) containing cOmplete™ protease inhibitor cocktail (Merck, Darmstadt, Germany) and 4 mM phenylmethylsulfonyl fluoride (Thermofisher Scientific). Following a 1-min centrifugation, 65 μl of supernatant was added to 20 μl of sample 4X Laemmli buffer. Total proteins were separated through a 10% SDS-polyacrylamide resolving gel. Then proteins were transferred to nitrocellulose membranes (Amersham™, Merck). Membranes were blocked for 1 h in the blocking solution (1X phosphate buffer saline, 0.1% Tween 20, 5% dry milk) and incubated overnight with primary antibodies at 4 °C. The following commercial primary antibodies were used: rabbit anti-TDP43 antibody (1/1000, 10782-2-AP, Proteintech, Manchester, UK), rabbit anti-BiP (1/700, SPC-180, StressMarq Biosciences, Victoria, Canada), mouse anti-ATP5α antibody (1/800, ab14748, abcam, Cambridge, UK). Human S1R protein was detected using a rabbit polyclonal antibody generated by Abliance (Compiègne, France) as previously described [20]). Secondary peroxidase-conjugated antibodies (1/5000, Jackson ImmunoResearch, Cambridge, UK) were incubated for 2 h in blocking solution. Chemiluminescence was revealed by using the Clarity™ Western ECL Blotting substrates (Bio-Rad, Marnes-la-Coquette, France) and the ChemiDoc Touch Imaging System (Bio-Rad). Quantitative analysis was performed using Fiji (Fiji Is Just ImageJ) software

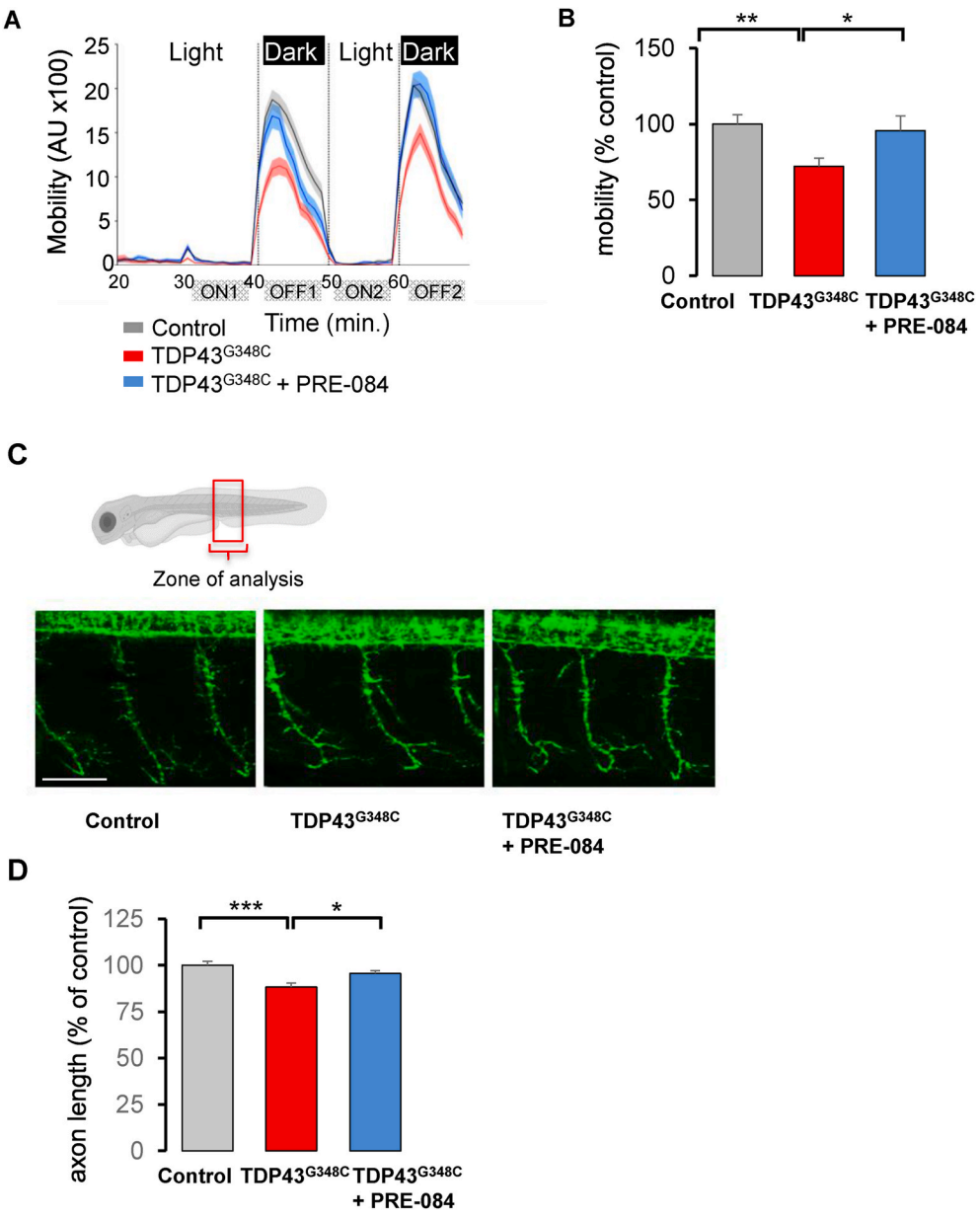

Fig. 2. PRE-084 ameliorated TDP43^{G348C}-larvae mobility and axonal projection. (**A**) Mobility of control larvae, larvae expressing TDP43^{G348C} alone or treated with 5 μM of PRE-084 during the light/dark phases in the VMR test. The mobility was measured during 1 min each. AU: arbitrary unit. (**B**) Quantitative analyses from (A) showing the relative mobility of controls, larvae expressing TDP43^{G348C} alone or treated with PRE-084. Data were the mean of the mobility during the two OFF periods minus ON periods (OFF1-ON1; OFF2-ON2). Relative mobility from >100 larvae was expressed as percent of control and presented as mean ± SEM. Statistical analysis was performed using ANOVA followed by Tukey's test (**p < 0.01; ***p < 0.001). (**C**) Representative photomicrographs showing three axonal projections in the zone of analysis. Scale bar: 50 μm. (**D**) Quantitative analyses of axonal projections (as shown in (C)) in control larvae or larvae expressing TDP43^{G348C} alone or treated with PRE-084. Data from 42 to 54 motor neurons were averaged and presented as mean ± SEM. Statistical analysis was performed using ANOVA followed by Tukey's test (*p < 0.05; ***p < 0.001).

[33].

2.6. Touch-escape test

The touch-escape assay quantifies the locomotor activity of zebrafish larvae consecutively to a mechanical stimulation [34]. Larvae that presented visible anomalies or deformities were not used for the experiment. At 5 dpf, individual zebrafish larva was transferred in the extremity of a longitudinal tank (L 17.5 × W 0.5 × H 1 cm) filled with 2.6 ml of zebrafish water and equipped with a graduated scale (Suppl. Fig. 1A). After an acclimatization of 30 s, application of tactile stimuli to the tail fin using a tip was carried out. The distance swam in 5 s was evaluated. The larva was then placed again at the extremity and two other assays were performed after a rest of 30 s between each session.

2.7. Visual motor response (VMR)

This test quantifies the mobility of zebrafish larvae in response to light/dark changes using infrared tracking system. At 5dpf, individual larvae are transferred in wells of 96 well plate (Whatman #7701-1651 square and flat bottom wells) with 250 μl of water and placed for 1 h in the incubator at 28 °C. Larvae that did not have swim bladders or presented visible physiological deformities were not used for the experiment. The box floor emitted by a light-controlling unit a white light (69–83 μW/cm^2 measured at λ 495 nm). The response to stimuli was recorded by an infra-red (IR) camera (25 frames/s). The activity of larvae was monitored by using an automated videotracking device (Zebrabox, ViewPoint, Lyon, France), employing a DinionXF 1/3-inch Monochrome camera (model BFLY-PGE-13H2M, FLIR) fitted with a fixed-angle megapixel lens (SR5014MP-5C, Seiko Optical, Tokyo, Japan). The experiment consisted in acclimating larvae to darkness for 30 min, then switching light ON for 10 min, then OFF during 10 min. This was repeated twice, giving a total experiment duration of 70 min. The amount of movement was measured for each larva in "actinteg" units. The "actinteg" value of Viewpoint software is defined as the sum of all image pixel changes detected during the time window (1 min) defined for the experiment. The values obtained in OFF were subtracted for each larva to their ON values in order to normalize with the basic

activity of each larva.

2.8. Unbranched axonal length measurements

Length of axon motor neurons was evaluated after immunostaining using mouse monoclonal antibody anti-ZNP1 (Developmental Studies Hybridoma, Iowa city, Iowa, USA). Larvae at 2 dpf were used since axonal projections of motor neurons are easily visible at this age. Fluorescent images of fixed larvae were taken using a confocal ZEISS 880 FastAi (Rueil Malmaison, France). Axonal projections from primary motor neurons at a defined location in the inter-somite segments were determined. Analysis of Z-stacks by confocal microscopy was performed on 3 axonal projections per zebrafish. The axonal length was determined by tracing the labeled axon from the spinal cord to the point where it branches using Fiji software [33]. Statistical analysis was performed on 15–19 zebrafishes per condition for the various conditions.

2.9. Oxygen consumption rate measured by seahorse technology

The oxygen consumption rate (OCR) of 5 dpf larvae was measured with a Seahorse XFe24 extracellular flux analyzer (Agilent, Santa Clara, California, USA). The Seahorse temperature was maintained at 28 °C. The larvae were placed individually in a well of a Seahorse XFe24 spheroid 24-well microplate, with 500 µl of water. A grid was placed on the larvae to maintain them at the bottom of the wells throughout the experiment. Two wells were kept empty per experiment and were considered as the "blank" condition. Measurements of total zebrafish OCR were performed according to the manufacturer's instructions. Five basal analysis cycles were recorded, then five cycles recorded after administration of oligomycin (20 µM final; Sigma Aldrich), five cycles after administration of carbonyl cyanide-*p*-trifluoromethoxyphenylhydrazone (FCCP) (8 µM; Sigma Aldrich) and eight cycles after rotenone + antimycin A (15 µM each; Sigma Aldrich). Oligomycin inhibits ATP synthase. FCCP is an uncoupling agent that collapses the proton gradient and disrupts the mitochondrial membrane potential. A mixture of rotenone, a complex I inhibitor, and antimycin A, a complex III inhibitor shuts down mitochondrial respiration. As a result, drugs enable the calculation of basal mitochondrial respiration, the maximal capacity of mitochondrial respiration and non-mitochondrial respiration, according to the Manufacturer's guide (Agilent).

2.10. Statistical analysis

Data were presented as mean ± standard error of the mean (SEM). Statistical analysis was conducted by using Prism GraphPad 8.3 software. Student's *t*-test was performed to compare two groups, while one-way ANOVA followed by Tukey's test was used for comparison between multiple groups. Statistical significance was reached if p values was <0.05.

3. Results

3.1. PRE-084 rescued locomotor and motor neuron defects of $TDP43^{G348C}$ zebrafish larvae

Locomotor behavior tests were first used to determine locomotor deficits induced by $TDP43^{G348C}$ overexpression. The touch-escape assay was used to quantify the locomotor performances consecutively to a mechanical stimulation at 5 dpf. While larvae expressing a control mCherry protein swam a similar distance in 5 s as compared to controls, larvae expressing $TDP43^{G348C}$ showed a significant reduced motor response (Fig. 1A). To provide a direct proof that a neuroprotective strategy could be based on S1R, a transgenic zebrafish overexpressing human S1R was generated (Suppl. Fig. 1C). In transgenic S1R larvae, $TDP43^{G348C}$ did not affect swimming escape response compared to

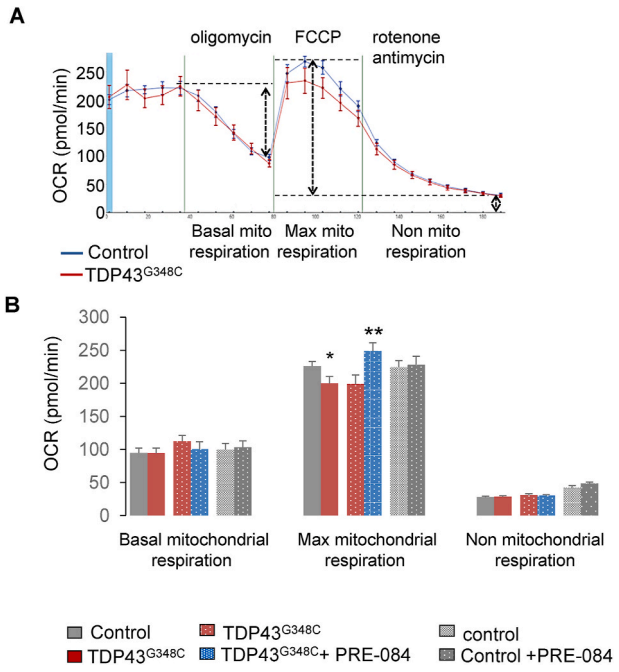

Fig. 3. PRE-84 boosted maximal mitochondrial respiration of $TDP43^{G348C}$-expressing larvae. (**A**) Oxygen consumption rate (OCR) was measured using the Seahorse system on control and $TDP43^{G348C}$ larvae. (**B**) Basal mitochondrial respiration, maximal capacity of mitochondrial respiration and non-mitochondrial respiration were measured on control and $TDP43^{G348C}$ larvae treated or not with PRE-084. Data from n = 18–33 larvae were presented as mean ± SEM. Statistical analysis was performed by the Student t-test (*$p < 0.05$; **$p < 0.01$).

controls (Fig. 1B). Overexpressing S1R alone had also no impact on the touch-escape response (Fig. 1B). Next, we examined the effect of the reference S1R agonist, PRE-084. Two concentrations of PRE-084, 5 and 10 µM; the drug being added to the bath water for 24 h between 4 and 5 dpf. Interestingly, the swimming distance of $TDP43^{G348C}$-expressing zebrafish was rescued after the treatment with PRE-084 at the two doses (Fig. 1C). To confirm the specificity of the protective effect of PRE-084, larvae were treated with PRE-084 alone or with the S1R antagonist, NE-100, at 5 µM each. Treatment with NE-100 significantly abolished the protective effect of PRE-084 (Fig. 1D). As control experiments, we observed that PRE-084 by itself had no impact on the locomotion of control larvae and NE-100 alone did not modify the locomotor behavior of $TDP43^{G348C}$ larvae (Suppl. Fig. 2). Another S1R agonist, SA4503, was tested in $TDP43^{G348C}$ larvae and again this treatment rescued the locomotor escape response (Fig. 1E).

We also performed the locomotor response to light intensity changes, using the visual motor response assay (VMR). Larvae are placed in a 96-well plate in a zebrabox and after 30 min, two consecutive periods of light onset (ON) and light offset (OFF) for 10 min each. Larvae showed increased locomotion during dark periods (Fig. 2A). The expression of $TDP43^{G348C}$ reduced the mobility of larvae during dark periods (Fig. 2B). The mean mobility significantly decreased by 28% in the presence of $TDP43^{G348C}$. More importantly, treatment with PRE-084 at 5 µM rescued the response of $TDP43^{G348C}$-expressing larvae in the VMR test (Fig. 2B).

Expression of $TDP43^{G348C}$ was reported to shorten motor neuron extension [35]. We therefore examined the axonal length of motor neurons on 2 dpf larvae. While in $TDP43^{G348C}$-expressing larvae the mean axon length was significantly reduced by 12%, PRE-084 treatment rescued this alteration (Fig. 2C and D). Altogether our results emphasized the beneficial effects of S1R activation in a zebrafish vertebrate model of ALS.

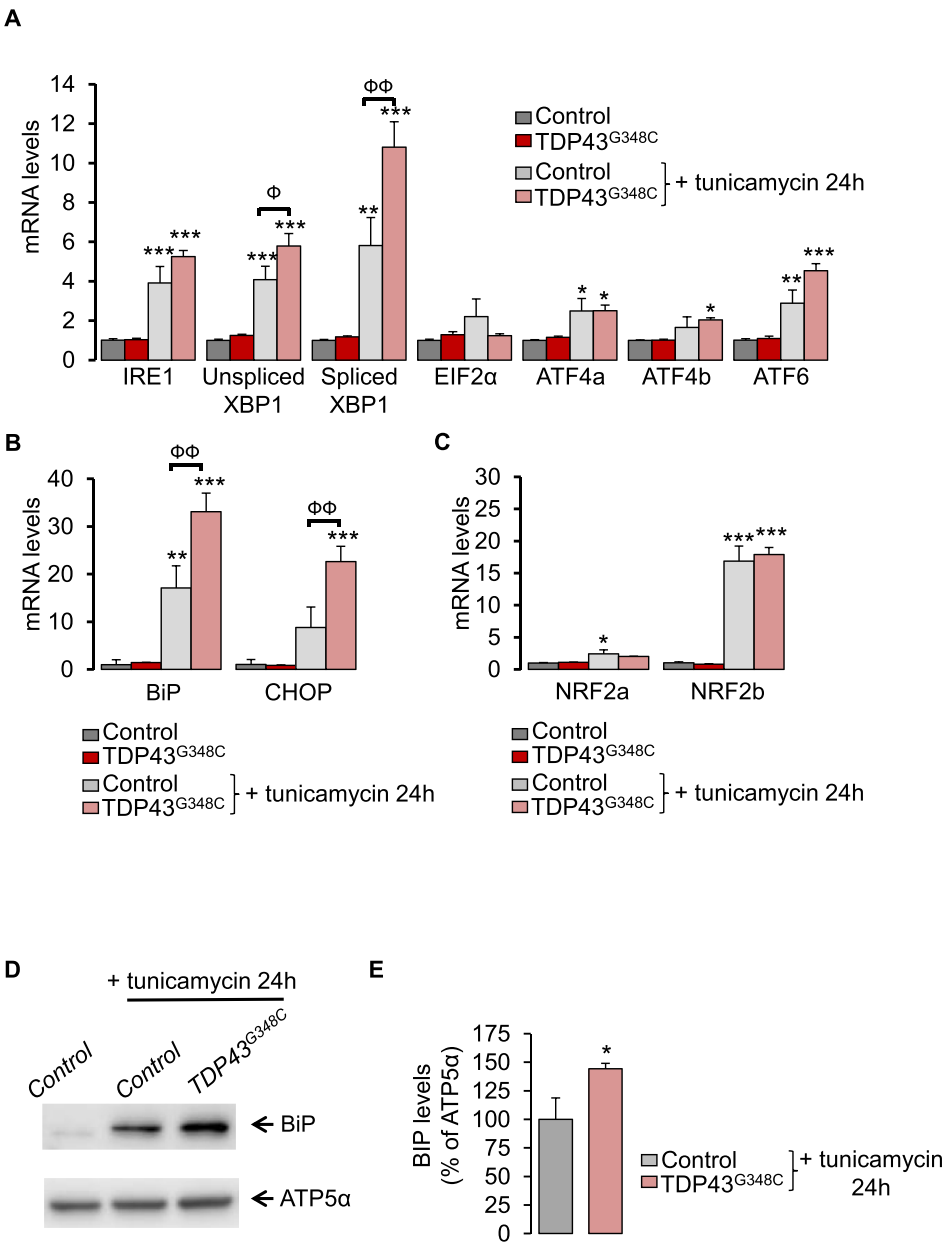

Fig. 4. TDP43^{G348C} increased sensitivity to ER stress. (**A**) Transcript levels were evaluated from control or TDP43^{G348C} larvae, treated or not with the ER stress inducer, tunicamycin, for 24 h. Data from n = 5 were presented as mean ± SEM. Statistical analysis was performed by using ANOVA followed by Tukey's test (*p < 0.05, **p < 0.01 and ***p < 0.001 versus control condition; Φp<0.05, ΦΦp<0.01). (**B**) As in (A) for UPR gene targets: *BiP* and *CHOP* (**p < 0.01 and ***p < 0.001 versus control condition; ΦΦp<0.01). (**C**) As in (A) for *NRF2* isoforms: *NRF2a* and *NRF2b* (*p < 0.05 and ***p < 0.001 versus control condition). (**D**) Western blot showing BiP and ATP5α protein levels from control or TDP43^{G348C} larvae treated or not with tunicamycin for 24 h. (**E**) Densitometric analysis of BiP protein levels in zebrafish larvae from (D). ATP5α was used as a reference to normalize BiP levels. Data from 5 independent samples were averaged and presented as mean ± SEM. Statistical analysis was performed using a Student's *t*-test (*p < 0.05).

3.2. PRE-084 ameliorated ATP production during high energy demand

Since S1R is a chaperone protein, we first investigated whether or not S1R activation by PRE-084 affected TDP43 levels. Western blot analyses revealed that PRE-084 did not affect expression of human TDP43 levels (Suppl. Fig. 3). Among its functions, S1R regulates energy production by mitochondria. Mitochondrial respiration activity was then evaluated by using a 24 plate-Seahorse XF analyzer (Agilent™). This system allows the measure on the whole zebrafish larvae of the basal mitochondrial activity to produce ATP, the maximal capacity of mitochondria to function and the non-mitochondrial respiration. The presence of TDP43^{G348C} significantly reduced the maximal mitochondrial respiration, suggesting a mitochondrial dysfunction during high energy demand (Fig. 3A and B). Of importance, PRE-084 treatment enhanced maximal mitochondrial respiration in TDP43^{G348C} context but not in control condition (Fig. 3B).

3.3. TDP43^{G348C} exacerbated tunicamycin-induced ER stress sensitivity

Abnormal accumulation of unfolded proteins in the ER, leads to an ER stress response, also termed the UPR. During unstressed conditions, the chaperone protein, GRP78/BiP, is associated to ER stress sensors (IRE1, PERK, ATF6), keeping them inactive. Upon ER stress, GRP78/BiP dissociates from these sensors resulting in the activation of the three UPR arms. As a consequence, this leads to the UPR characterized by increased levels of chaperone proteins like GRP78/BiP itself. However, under persistent ER stress, the normal functions of the ER fail to recover and results in apoptosis, as characterized by overexpression of the transcription factor C/EBP homologous protein (CHOP). Impact of TDP43 on ER stress has been poorly studied *in vivo*.

We have investigated levels of ER stress response genes by using RT-qPCR on 5 dpf zebrafish larvae. TDP43^{G348C} expression did not modify mRNA levels of the three canonical UPR pathways: i) IRE1 and spliced (active) or unspliced forms of Xbp1, ii) PERK/EIF2α and ATF4 isoforms (ATF4a/ATF4b) and iii) ATF6 (Fig. 4A). Next, we used tunicamycin at 2

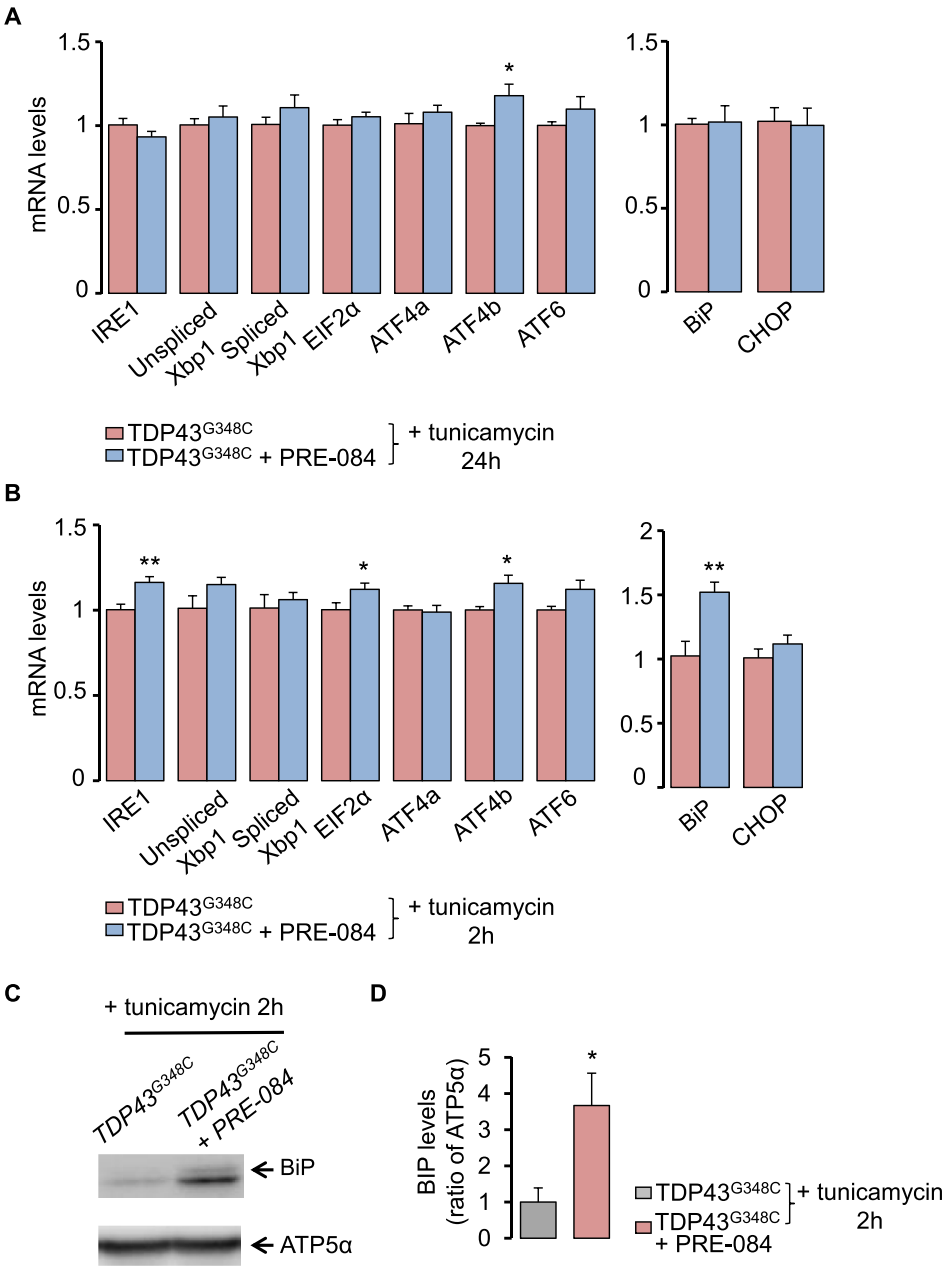

Fig. 5. PRE-084 enhanced ER stress response in TDP43^{G348C}-zebrafish. (**A**) Transcript levels of UPR genes in TDP43^{G348C} larvae, treated or not with PRE-084 after an ER stress induction with tunicamycin for 24 h. Data from n = 8–9 were presented as mean ± SEM. Statistical analysis was performed by using Student t-test (*p < 0.05). (**B**) As in (A) but after an ER stress induction for 2 h. Data from n = 6–7 were presented as mean ± SEM. Statistical analysis was performed by using Student t-test (*p < 0.05; **p < 0.01). (**C**) Western blot showing BiP and ATP5α protein levels larvae expressing TDP43^{G348C} treated or not with PRE-084 after 2 h with tunicamycin condition. (**D**) Quantitative analysis of BiP protein levels in zebrafish larvae from (C). ATP5α was used as a reference to normalize BiP levels. Data from 8 to 9 independent samples were averaged and presented as mean ± SEM Statistical analysis was performed by using Student t-test (*p < 0.05).

μg/ml for 24 h to induce ER stress and subsequently, the overexpression of UPR genes as shown in Fig. 4A. Likewise, levels of downstream UPR genes, *BiP* and *CHOP*, were stimulated by tunicamycin (Fig. 4B). Noteworthy one canonical UPR pathway was significantly overwhelmed by the presence of TDP43^{G348C} during ER stress: the IRE1/Xbp1 cascade (Fig. 4A). The unspliced (inactive)/spliced (active) ratio of *Xbp1* was found significantly increased (+33%, p < 0.05) in TDP43^{G348C}-expressing larvae. In parallel, TDP43^{G348C} further boosted *BiP* and *CHOP* upregulation in the presence of tunicamycin (Fig. 4B). Thus, mutant TDP43 increased the vulnerability to ER stress *in vivo*. At the protein level, while TDP43^{G348C} did not modify BiP protein expression alone (Suppl. Fig. 4), it further enhanced BiP protein expression in the presence of tunicamycin (Fig. 4D and E and Suppl. Fig. 5).

Antioxidant NRF2 signalling pathway and ER stress response are closely related. In particular, PERK/EIF2α not only phosphorylates and activates NRF2 but also ATF4 was shown to promote *NRF2* transcription [36–38]. We thus examined mRNA levels of the two NRF2 isoforms: *NRF2a* and *NRF2b*. Treatment of 5 dpf wild-type larvae with tunicamycin for 24 h led to a 17-fold increase in *NRF2b* but had no effect on *NRF2a* transcript levels (Fig. 4C). TDP43^{G348C} did not affect levels of *NRF2* levels in the presence or not of tunicamycin as compared to control.

3.4. PRE-084 stimulated ER stress response in TDP43^{G348C} larvae

To better understand how S1R activation may prevent TDP43 toxicity, we studied the impact of PRE-084 on ER stress response after exposure of larvae with tunicamycin. Larvae were treated with 5 μM PRE-084 at 4 dpf for 24 h and were analyzed for RNA levels of canonical UPR genes. After treatment with tunicamycin for 24 h, PRE-084 only increased levels of *ATF4b* transcript in TDP43^{G348C}-expressing larvae (Fig. 5A). Expression of UPR downstream genes, *BiP* and *CHOP*, remained unchanged (Fig. 5A). To determine if changes also occur and are more pronounced at shorter term during ER stress, a treatment of 2 h was performed with tunicamycin (Fig. 5B). In this condition, PRE-084 revealed significant increase in mRNA encoding *ATF4b* but also *IRE1*,

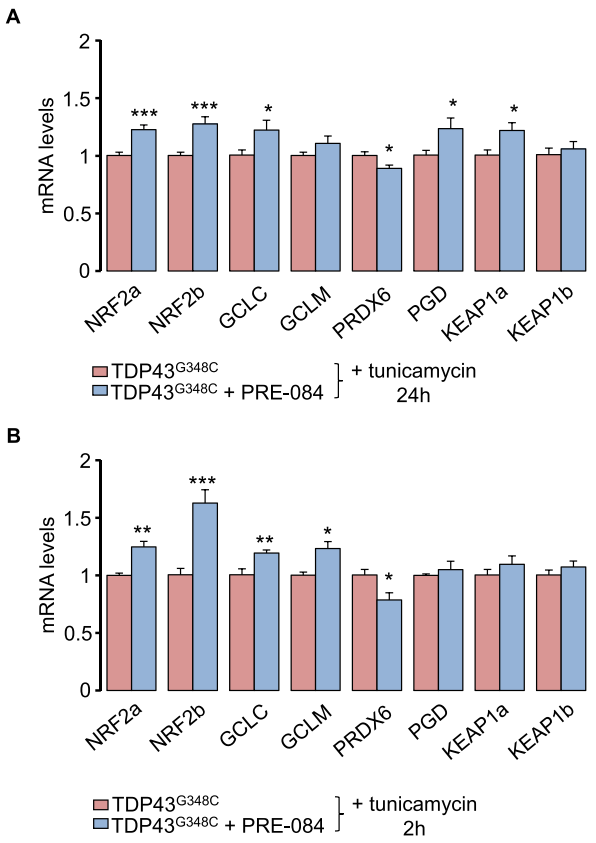

Fig. 6. PRE-084 boosted NRF2 signalling cascade and alleviates TDP43^{G348C} toxicity. (**A and B**) RNA expression levels of *NRF2* and its targets: *GCLC*, *GCLM*, *PRDX6* and *PGD* in TDP43^{G348C} larvae treated or not with PRE-084 after an ER stress induction with tunicamycin for 24 h (A) or 2 h (B). Data from n = 8–9 (24 h) and n = 6–7 (2 h) were presented as mean ± SEM. Statistical analysis was performed by the Student t-test (*p < 0.05; **p < 0.01; ***p < 0.001).

EIF2α and *BiP* (Fig. 5B). Altogether this data indicates that PRE-084 may have beneficial effects by boosting UPR signalling pathway. Analyses at protein levels further showed that PRE-084 increased by 3.6-fold BiP levels in the TDP43 context (Fig. 5C and D).

3.5. PRE-084 activated antioxidant NRF2 pathway in TDP43^{G348C} larvae

Next, we examined the effect of PRE-084 on NRF2 signalling pathway that controls antioxidant pathway. Transcript levels of *NRF2a/NRF2b* were found increased in the presence of PRE-084 with tunicamycin for 2 h or 24 h (Fig. 6A). NRF2 is known to activate expression of antioxidant key genes in glutathione-based system (*GCLC*, *GCLM*), thioredoxin-based system (*PRDX6*), NADPH-generating enzyme 6-phosphogluconate dehydrogenase (*PGD*), as well as on its inhibitor *KEAP1*. Consecutively to a 24 h treatment with tunicamycin, PRE-084 elevated mRNA levels of *GCLC*, *PDG* and *KEAP1a* isoform but to reduce *PRDX6* levels (Fig. 6A). At a shorter term of 2 h, PRE-084 enhanced expression of *GCLC* and *GCLM* but reduced that of PRDX6 (Fig. 6B). The impact of PRE-084 on NRF2 levels was further studied in physiological condition. Interestingly, treatment of control larvae with PRE-084 for 2 h and 24 h increased levels of *NRF2a/NRF2b* and *NRF2b* transcripts, respectively (Suppl. Fig. 6). Altogether these observations strongly suggest a role of NRF2 signalling in the beneficial impact of PRE-084.

3.6. Enhancing NRF2 expression ameliorated locomotor defects of TDP43^{G348C} larvae

To further demonstrate that increasing *NRF2* levels confers protection against TDP43 toxicity, we treated our ALS zebrafish model with sulforaphane, that was previously used to activate NRF2 signalling in zebrafish [39,40]. A treatment with 40 μM sulforaphane was sufficient to enhance mRNA expression of *NRF2b* as well as its targets *GCLC*, *GCLM*, *PDG* and *PRDX6* (Fig. 7A and B). Surprisingly, *NRF2a* mRNA levels were found decreased. Noteworthy, sulforaphane rescued the locomotor response of TDP43^{G348C}- expressing zebrafish in the touch-escape test (Fig. 7C). Finally, we directly tested the impact of injected *NRF2* zebrafish transcript together with TDP43^{G348C} mRNA (Fig. 7D). We found a rescue of the locomotor escape response of TDP43^{G348C}-expressing zebrafish (Fig. 7D).

4. Discussion

The interest of S1R in ALS is fostered by the fact that mutations in the gene result in juvenile cases of ALS [21,22]. Moreover, in the SOD1^{G93A} mouse model of ALS, several S1R agonists were found to slow the progression of neuronal alterations or behavioral phenotype [24–27]. Altogether these data made S1R agonists a promisingly potent therapeutic tool to counteract ALS pathology. However, it is now imperative to further validate the therapeutic concept in other ALS contexts and to ascertain their mode of action. By using genetic approaches in *Drosophila*, we previously demonstrated that overexpressing S1R reversed climbing deficits of TDP43-expressing flies [28]. We here showed in a vertebrate model that locomotion of zebrafish overexpressing human S1R are less affected by mutant TDP43 than controls. The purpose of the present study was to provide the proof of concept that the S1R activation by the agonist, PRE-084, is efficient to counteract TDP43 toxicity. While expression of mutant TDP43 leads to locomotor defects, PRE-084 treatment rescues performances not only in the touch-escape test but also the VMR. Moreover, we dissected some of the mechanisms underlying PRE-084 protective effects. Treatment with the agonist ameliorates maximal mitochondrial respiration in the TDP43 context. One the other hand, we demonstrated that TDP43^{G348C} exacerbates ER stress by enhancing response to tunicamycin, resulting in increased levels of ER stress chaperone BiP and pro-apoptotic factor CHOP. Interestingly, PRE-084 treatment in the same condition further heightens *BiP* mRNA levels but not *CHOP*. Moreover PRE-084 stimulates EIF2α/ATF4 and NRF2 signalling, both known to promote antioxidant protection during ER stress. To further validate the protective effect of NRF2 in TDP43 context, we showed that overexpressing *NRF2* alleviates locomotor defects to mechanical stimulation of TDP43^{G348C} zebrafish. Additionally, we looked for potential benefits of sulforaphane, well known to enhance NRF2 signalling pathway, and again we found an amelioration of the touch-escape response of zebrafish expressing TDP43^{G348C}. Altogether, these findings highlight the beneficial impact of activating S1R in ALS pathogenesis, boosting ER stress response and antioxidant cascade.

The preferential localization of S1R at the ER-mitochondria interface supports its action on mitochondria. At this domain its interaction with IP3R type 3 adapts calcium transfer from ER to mitochondria and thereby modulates production of NADH cofactor by intra-mitochondrial dehydrogenases [41]. The activation of these enzymes by calcium is considered important to stimulate mitochondrial respiration and hence matches ATP supply with increased energetic needs [42]. We showed that PRE-084 stimulates maximal oxidative mitochondrial respiration that was significantly reduced by the presence of TDP43^{G348C}. In contrast, basal ATP-dependent respiration remained unchanged in the presence of TDP43^{G348C} and/or PRE-084. It was previously reported that TDP43 may have a direct impact on mitochondria functioning, since cytoplasmic TDP43 could accumulate on the inner mitochondrial membrane and reduce complex I assembly thereby impairing ATP

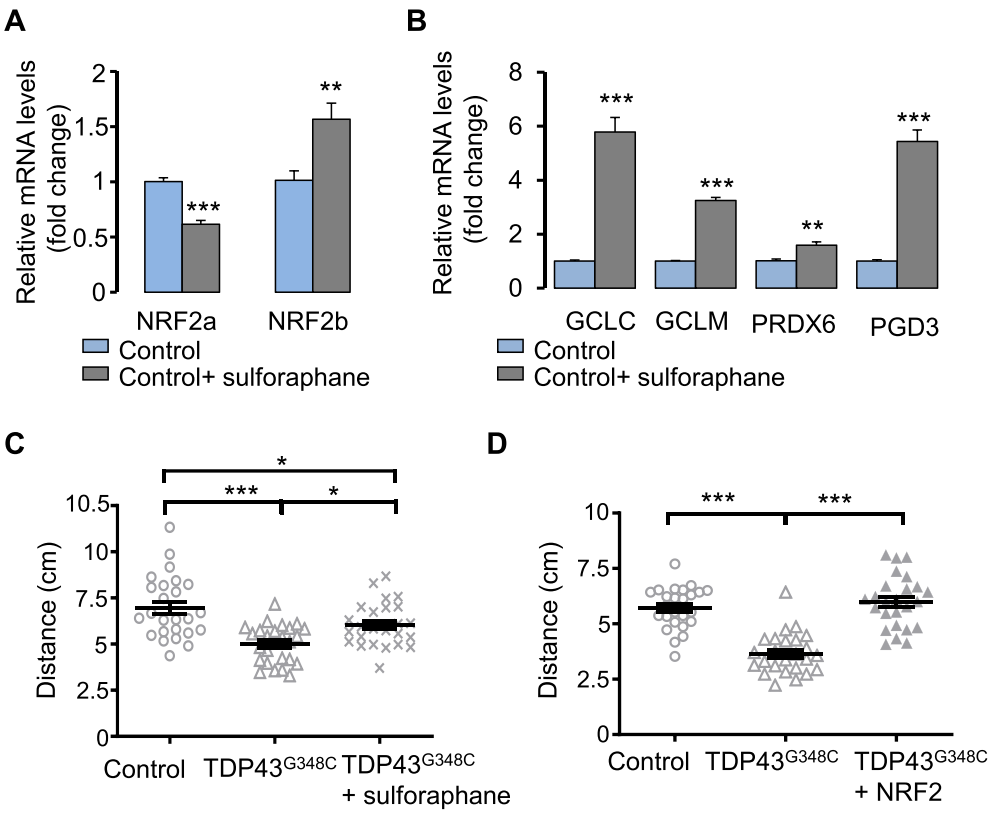

Fig. 7. Increasing *NRF2* levels reduced TDP43 toxicity. (**A**) RNA expression levels of *NRF2* in larvae treated or not with sulforaphane. Data from n = 6 were presented as mean ± SEM. Statistical analysis was performed by the Student t-test (**p < 0.01; ***p < 0.001). (**B**) RNA expression levels of NRF2 targets: *GCLC*, *GCLM*, *PRDX6* and *PGD* in larvae treated or not with sulforaphane. Data from n ≥ 5 were presented as mean ± SEM. Statistical analysis was performed by the Student t-test (**p < 0.01; ***p < 0.001). (**C**) Touch-escape response of control larvae or larvae expressing $TDP43^{G348C}$ and treated or not with sulforaphane. Data from 25 were averaged and presented as mean ± SEM. Statistical analysis was performed by Tukey's test (*p < 0.05; ***p < 0.001). (**D**) Touch-escape response of control larvae or larvae expressing $TDP43^{G348C}$ alone or with NRF2. Data from 25 larvae were averaged and presented as mean ± SEM. Statistical analysis was performed using ANOVA followed by Tukey's test (***p < 0.001).

production [43]. Moreover, S1R agonists, including PRE-084, were found to directly potentiate complex I activity and mitochondrial respiration in physiological and pathological conditions [44]. Thus, S1R activation may confer protection by restoring mitochondrial respiratory capacity to fit with high energetic demand in TDP43 context. However, TDP43 toxicity results from a plethora of altered cellular processes, suggesting that rescuer effect of S1R may not solely be due to increased mitochondrial respiration.

In stress condition, S1R can activate the unfolded protein response, by acting on two UPR cascades: IXBP1 and ATF4 pathways [12–14]. Whether wild-type or mutant TDP43 triggers ER stress is still under debate [45]. Using NSC34 cells, it was found that TDP43 transfection did not activate IRE1/XBP1, ATF6 or PERK/ATF4 pathways while CHOP levels were increased [46]. Moreover, in HEK293 and primary motor neurons, mutant TDP43 failed to modify levels of spliced XBP1 and BiP [47], and even in rat forebrain neurons the authors noticed a decreased levels of unspliced/spliced XBP1 [48]. In contrast other studies in Neuro2a cells showed upregulation of XBP1, ATF6 and CHOP [49] while in SH-SY5Y cells they described higher levels of ATF4 and the ER stress effectors, BiP and CHOP [50,51]. All these discrepancies may be due to the different mutations and cell models that have been used and even likely the time-points of the observation. We showed here that induction of ER stress by tunicamycin increased transcript levels of all UPR genes but, more importantly, led to the higher exacerbation rate of IRE1/XBP1 cascade in $TDP43^{G348C}$ condition. This was accompanied by enhanced overexpression of *BiP* and *CHOP*, suggesting a higher vulnerability to ER stress in the presence of $TDP43^{G348C}$. BiP promotes survival by alleviating accumulation of misfolded proteins while CHOP activates apoptosis when ER stress is persisting (For reviews see [52,53]). CHOP expression can be activated by both ATF4 and ATF6 ER stress arms [53]. In ER stress conditions, we showed that PRE-084 treatment further enhanced *BiP* but not *CHOP* levels and upstream significantly increased mRNA levels of *IRE1*, *EIF2α* and *ATF4b*. In previous work in a S1R deficient zebrafish line, transcript levels of *IRE1* and PERK-related effectors like *ATF4* were found decreased [54]. Also, *ATF4* gene expression decreased after S1R silencing in transduced siRNA neurons [14]. We here provide evidence that, conversely, S1R activation can further increase UPR genes, *IRE1* and *ATF4*, as well as the pro-survival effector *BiP*.

Besides ER stress, our data indicate that S1R fulfils a key role in activation of defense against oxidative stress. In physiological conditions, KEAP1 binds NRF2 and then targets NRF2 for ubiquitination and degradation by the ubiquitin proteasome system. In contrast during oxidative stress NRF2-KEAP1 interaction is interrupted and NRF2 translocates to nucleus to activate expression of antioxidant genes. So far it has been reported that i) silencing S1R decreased NRF2 protein levels and led to oxidative stress in retinal cone cells, ii) S1R activation by ligands increased levels of NRF2 and NRF2-regulated antioxidant targets in retinal photoreceptors and Müller glial cells and iii) S1R colocalizes with NRF2 in photoreceptor cells, suggesting that NRF2 may be a direct target of S1R [15–17,55]. To date, analyses were performed mostly in retina and it is of interest to determine if the effect of S1R on NRF2 is a common mechanism. We are here demonstrating that PRE-084 enhances *NRF2* gene expression in physiological condition and in tunicamycin-induced stress. The impact on NRF2 targets seems to depend on the exposure time to tunicamycin, first affecting glutathione metabolism then NADPH levels with PGD and KEAP1 as negative feedback. The downregulation of *PRDX6* mRNA is in accordance with a direct gene regulation of this peroxiredoxin by S1R since silencing S1R was previously reported to upregulate PRDX6 transcripts, although how remains to be established [14]. Impact of S1R on NRF2 may be one of the most significant mechanism in the multifaceted neuroprotective action of S1R against TDP43 toxicity. Accordingly, increasing *NRF2* levels in zebrafish by sulforaphane and more directly by *NRF2* RNA injection both rescue locomotor defects induced by mutant TDP43. It is noteworthy that while sulforaphane and PRE-084 increase similarly *NRF2b* mRNA levels, the impact on transcript levels of NRF2-regulated targets is much more pronounced after sulforaphane treatment. Both drugs may

impact NRF2 signalling pathway through different mechanisms and not solely on transcript expression, among which phosphorylation by kinases and nuclear translocation of NRF2 protein are critical. Of interest, NRF2 was found to colocalize with S1R in photoreceptor cells, suggesting that NRF2 may be a direct target of S1R [55]. Future investigations should address the significance of this interaction in physiological condition or after activation by PRE-084. Moreover, we previously reported that S1R overexpression rescued the nucleocytoplasmic transport deficit caused by the ALS mutation in C9orf72 by stabilizing nuclear pore proteins and restoring the Ran gradient across nuclear membrane, that is essential for the nuclear import of RNA and proteins [20]. Since mutant TDP43 was also reported to alter nucleocytoplasmic transport [56], another alternative to explore is that PRE-084 may ameliorate nucleocytoplasmic transport of mRNA encoding NRF2 targets.

Altogether our data highlight the importance of NRF2 but also ATF4 in the beneficial impact of S1R activation. In general, ATF4 and NRF2 bind to their respective response elements, C/EBP-ATF response element (CARE) sequences and antioxidant responsive element (ARE), respectively, in response to distinct cellular stress. However, ATF4 is also described as part of the integrated stress response modulating crucial biological processes such as obviously ER stress but also antioxidant response and mitochondrial quality control [37,57,58]. Gene expressions of *ATF4* and *NRF2* is even intimately related, regulating each other [37,38,59,60]. Moreover, NRF2 form homodimers or heterodimers with other factors to stimulate targets. Several lines of evidence now indicate that ATF4 and NRF2 cooperatively stimulate genes controlling antioxidative defence, notably by forming heterodimers [36,61,62]. In future studies it would be very interesting to use morpholinos to downregulate NRF2 and ATF4, alone or together, to provide direct evidence of the synergic role of NRF2 and ATF4 in PRE-084-induced neuroprotection. While more work is needed to clarify all the mechanisms underlying S1R neuroprotection in TDP43 proteinopathy, our study confirmed the high therapeutic value of S1R agonists in ALS. An important issue in future investigations would be to understand the potential impact of S1R on the nucleocytoplasmic transport of NRF2 and its targets that has not been yet investigated in the TDP43 context.

Funding

This work was supported by a grant from the Association Française contre les Myopathies (AFM Téléthon; grant 23667).

Declaration of competing interest

The Authors declare to have no conflict of interest.

Data availability

Data will be made available on request.

Acknowledgement

We greatly thank Dr. Pierre Drapeau (University of Montreal) for providing us with thepCS2+TDP43^{G348C} plasmid, Dr. Georges Lutfalla (LPHI, Montpellier, France) for the PCS2+ mCherry plasmid and Pr. Masayuki Yamamoto (University of Tsukuba, Japan) for the pCS2+ NRF2 plasmid. We acknowledge the ZebraSens zebrafish phenotyping platform at MMDN (Montpellier, France) and the qPHd quantitative PCR platform at University of Montpellier (Montpellier, France). We also thank Philippe Clair for technical advices on RtqPCR, Cyril Beuvry and Dr. Pierre Charnet (IBMM, Montpellier, France) for the design of the touch-escape device and Dr Yoan Arribat (IRMB, Montpellier, France) for helpful advice regarding ZNP1 immunostaining.

Appendix A. Supplementary data

Supplementary data to this article can be found online at https://doi.org/10.1016/j.redox.2022.102542.

References

[1] R.G. Miller, J.D. Mitchell, D.H. Moore, Riluzole for amyotrophic lateral sclerosis (ALS)/motor neuron disease (MND), Cochrane Database Syst. Rev. 3 (2012), CD001447, https://doi.org/10.1002/14651858.CD001447.pub3.
[2] B. Oskarsson, T. Gendron, N. Staff, Amyotrophic lateral sclerosis: an update for 2018, Mayo Clin. Proc. 93 (2018), https://doi.org/10.1016/j.mayocp.2018.04.007.
[3] B. Khalil, J.-C. Liévens, Mitochondrial quality control in amyotrophic lateral sclerosis: towards a common pathway? Neural Regen. Res. 12 (2017) 1052–1061, https://doi.org/10.4103/1673-5374.211179.
[4] F. Laferriere, M. Polymenidou, Advances and challenges in understanding the multifaceted pathogenesis of amyotrophic lateral sclerosis, Swiss Med. Wkly. 145 (2015), w14054, https://doi.org/10.4414/smw.2015.14054.
[5] T. Arai, M. Hasegawa, H. Akiyama, K. Ikeda, T. Nonaka, H. Mori, D. Mann, K. Tsuchiya, M. Yoshida, Y. Hashizume, T. Oda, TDP-43 is a component of ubiquitin-positive tau-negative inclusions in frontotemporal lobar degeneration and amyotrophic lateral sclerosis, Biochem. Biophys. Res. Commun. 351 (2006) 602–611, https://doi.org/10.1016/j.bbrc.2006.10.093.
[6] A.N. Coyne, B.L. Zaepfel, D.C. Zarnescu, Failure to deliver and translate—new insights into RNA dysregulation in ALS, Front. Cell. Neurosci. 11 (2017), https://doi.org/10.3389/fncel.2017.00243.
[7] T. Maurice, Bi-phasic dose response in the preclinical and clinical developments of sigma-1 receptor ligands for the treatment of neurodegenerative disorders, Expet Opin. Drug Discov. 16 (2021) 373–389, https://doi.org/10.1080/17460441.2021.1838483.
[8] T. Hayashi, T. Maurice, T.P. Su, Ca(2+) signaling via sigma(1)-receptors: novel regulatory mechanism affecting intracellular Ca(2+) concentration, J. Pharmacol. Exp. Therapeut. 293 (2000) 788–798.
[9] T. Hayashi, T.-P. Su, Sigma-1 receptor chaperones at the ER-mitochondrion interface regulate Ca(2+) signaling and cell survival, Cell 131 (2007) 596–610, https://doi.org/10.1016/j.cell.2007.08.036.
[10] H. Tagashira, M.S. Bhuiyan, N. Shioda, K. Fukunaga, Fluvoxamine rescues mitochondrial Ca2+ transport and ATP production through σ(1)-receptor in hypertrophic cardiomyocytes, Life Sci. 95 (2014) 89–100, https://doi.org/10.1016/j.lfs.2013.12.019.
[11] G. Alonso, V. Phan, I. Guillemain, M. Saunier, A. Legrand, M. Anoal, T. Maurice, Immunocytochemical localization of the sigma(1) receptor in the adult rat central nervous system, Neuroscience 97 (2000) 155–170, https://doi.org/10.1016/s0306-4522(00)00014-2.
[12] T. Mori, T. Hayashi, E. Hayashi, T. Su, Sigma-1 receptor chaperone at the ER-mitochondrion interface mediates the mitochondrion-ER-nucleus signaling for cellular survival, PLoS One 8 (2013), https://doi.org/10.1371/journal.pone.0076941.
[13] T.-P. Su, T.-C. Su, N. Yoki, T. Shang-Yi, The sigma-1 receptor as a pluripotent modulator in living systems, Trends Pharmacol. Sci. 37 (2016) 262–278, https://doi.org/10.1016/j.tips.2016.01.003.
[14] S.-Y. Tsai, R.K. Rothman, T.-P. Su, Insights into the Sigma-1 receptor chaperone's cellular functions: a microarray report, Synapse 66 (2012) 42–51, https://doi.org/10.1002/syn.20984.
[15] J. Wang, A. Shanmugam, S. Markand, E. Zorrilla, V. Ganapathy, S.B. Smith, Sigma 1 receptor regulates the oxidative stress response in primary retinal Müller glial cells via NRF2 signaling and system xc(-), the Na(+)-independent glutamate-cystine exchanger, Free Radic. Biol. Med. 86 (2015) 25–36, https://doi.org/10.1016/j.freeradbiomed.2015.04.009.
[16] J. Wang, J. Zhao, X. Cui, B.A. Mysona, S. Navneet, A. Saul, M. Ahuja, N. Lambert, I. G. Gazaryan, B. Thomas, K.E. Bollinger, S.B. Smith, The molecular chaperone sigma 1 receptor mediates rescue of retinal cone photoreceptor cells via modulation of NRF2, Free Radic. Biol. Med. 134 (2019) 604–616, https://doi.org/10.1016/j.freeradbiomed.2019.02.001.
[17] H. Xiao, J. Wang, A. Saul, S.B. Smith, Comparison of neuroprotective effects of monomethylfumarate to the sigma 1 receptor ligand (+)-Pentazocine in a murine model of retinitis pigmentosa, Invest. Ophthalmol. Vis. Sci. 61 (2020) 5, https://doi.org/10.1167/iovs.61.3.5.
[18] U.B. Chu, A.E. Ruoho, Biochemical pharmacology of the sigma-1 receptor, Mol. Pharmacol. 89 (2016) 142–153, https://doi.org/10.1124/mol.115.101170.
[19] S.-Y.A. Tsai, J.-Y. Chuang, M.-S. Tsai, X.-F. Wang, Z.-X. Xi, J.-J. Hung, W.-C. Chang, A. Bonci, T.-P. Su, Sigma-1 receptor mediates cocaine-induced transcriptional regulation by recruiting chromatin-remodeling factors at the nuclear envelope, Proc. Natl. Acad. Sci. U. S. A. 112 (2015) E6562–E6570, https://doi.org/10.1073/pnas.1518894112.
[20] P. Lee, J.-C. Liévens, S. Wang, J. Chuang, B. Khalil, H. Wu, W.-C. Chang, T. Maurice, T.-P. Su, Sigma-1 receptor chaperones rescue nucleocytoplasmic transport deficit seen in cellular and Drosophila ALS/FTD models, Nat. Commun. 11 (2020), https://doi.org/10.1038/s41467-020-19396-3.
[21] A. Al-Saif, F. Al-Mohanna, S. Bohlega, A mutation in sigma-1 receptor causes juvenile amyotrophic lateral sclerosis, Ann. Neurol. 70 (2011) 913–919, https://doi.org/10.1002/ana.22534.

[22] S. Watanabe, H. Ilieva, H. Tamada, H. Nomura, O. Komine, F. Endo, S. Jin, P. Mancias, H. Kiyama, K. Yamanaka, Mitochondria-associated membrane collapse is a common pathomechanism in SIGMAR1- and SOD1-linked ALS, EMBO Mol. Med. 8 (2016) 1421–1437, https://doi.org/10.15252/emmm.201606403.
[23] T.A. Mavlyutov, M.L. Epstein, Y.I. Verbny, M.S. Huerta, I. Zaitoun, L. Ziskind-Conhaim, A.E. Ruoho, Lack of sigma-1 receptor exacerbates ALS progression in mice, Neuroscience 240 (2013) 129–134, https://doi.org/10.1016/j.neuroscience.2013.02.035.
[24] R. Mancuso, S. Oliván, A. Rando, C. Casas, R. Osta, X. Navarro, Sigma-1R agonist improves motor function and motoneuron survival in ALS mice, Neurotherapeutics 9 (2012) 814–826, https://doi.org/10.1007/s13311-012-0140-y.
[25] Y. Ono, Tanaka, M. Takata, Y. Nagahara, Y. Noda, K. Tsuruma, M. Shimazawa, I. Hozumi, H. Hara, SA4503, a sigma-1 receptor agonist, suppresses motor neuron damage in in vitro and in vivo amyotrophic lateral sclerosis models, Neurosci. Lett. 559 (2014) 174–178, https://doi.org/10.1016/j.neulet.2013.12.005.
[26] A. Ionescu, T. Gradus, T. Altman, R. Maimon, N. Saraf Avraham, M. Geva, M. Hayden, E. Perlson, Targeting the sigma-1 receptor via pridopidine ameliorates central features of ALS pathology in a SOD1G93A model, Cell Death Dis. 10 (2019) 210, https://doi.org/10.1038/s41419-019-1451-2.
[27] N. Gaja-Capdevila, N. Hernández, X. Navarro, M. Herrando-Grabulosa, Sigma-1 receptor is a pharmacological target to promote neuroprotection in the SOD1G93A ALS mice, Front. Pharmacol. 12 (2021), 780588, https://doi.org/10.3389/fphar.2021.780588.
[28] S. Couly, B. Khalil, V. Viguier, J. Roussel, T. Maurice, J.-C. Liévens, Sigma-1 receptor is a key genetic modulator in amyotrophic lateral sclerosis, Hum. Mol. Genet. 29 (2020) 529–540, https://doi.org/10.1093/hmg/ddz267.
[29] K. Kawakami, Transposon tools and methods in zebrafish, Dev. Dynam. 234 (2005) 244–254, https://doi.org/10.1002/dvdy.20516.
[30] T. Bonifacino, R.A. Zerbo, M. Balbi, C. Torazza, G. Frumento, E. Fedele, G. Bonanno, M. Milanese, Nearly 30 Years of animal models to study amyotrophic lateral sclerosis: a historical overview and future perspectives, Int. J. Mol. Sci. 22 (2021), 12236, https://doi.org/10.3390/ijms222212236.
[31] L. Li, M. Kobayashi, H. Kaneko, Y. Nakajima-Takagi, Y. Nakayama, M. Yamamoto, Molecular evolution of Keap1. Two Keap1 molecules with distinctive intervening region structures are conserved among fish, J. Biol. Chem. 283 (2008) 3248–3255, https://doi.org/10.1074/jbc.M708702200.
[32] K.J. Livak, T.D. Schmittgen, Analysis of relative gene expression data using real-time quantitative PCR and the 2−ΔΔCT method, Methods 25 (2001) 402–408, https://doi.org/10.1006/meth.2001.1262.
[33] J. Schindelin, I. Arganda-Carreras, E. Frise, V. Kaynig, M. Longair, T. Pietzsch, S. Preibisch, C. Rueden, S. Saalfeld, B. Schmid, J.-Y. Tinevez, D. James White, V. Hartenstein, K. Eliceiri, P. Tomancak, A. Cardona, Fiji: an open-source platform for biological-image analysis, Nat. Methods 9 (2012) 676–682, https://doi.org/10.1038/nmeth.2019.
[34] L. Crouzier, E. Richard, C. Diez, H. Alzaeem, M. Denus, N. Cubedo, T. Delaunay, E. Glendenning, S. Baxendale, J.-C. Liévens, T. Whitfield, T. Maurice, B. Delprat, Morphological, behavioral and cellular analyses revealed different phenotypes in Wolfram syndrome wfs1a and wfs1b zebrafish mutant lines, Hum. Mol. Genet. 31 (2022) 2711–2727, https://doi.org/10.1093/hmg/ddac065.
[35] A. Vaccaro, S.A. Patten, D. Aggad, C. Julien, C. Maios, E. Kabashi, P. Drapeau, J. A. Parker, Pharmacological reduction of ER stress protects against TDP-43 neuronal toxicity in vivo, Neurobiol. Dis. 55 (2013) 64–75, https://doi.org/10.1016/j.nbd.2013.03.015.
[36] S. Kasai, S. Shimizu, Y. Tatara, J. Mimura, K. Itoh, Regulation of Nrf2 by mitochondrial reactive oxygen species in physiology and pathology, Biomolecules 10 (2020) E320, https://doi.org/10.3390/biom10020320.
[37] S. Kasai, H. Yamazaki, K. Tanji, M. Engler, T. Matsumiya, K. Itoh, Role of the ISR-ATF4 pathway and its cross talk with Nrf2 in mitochondrial quality control, J. Clin. Biochem. Nutr. 64 (2019), https://doi.org/10.3164/jcbn.18-37.
[38] C. Sarcinelli, H. Dragic, M. Piecyk, V. Barbet, C. Duret, A. Barthelaix, C. Ferraro-Peyret, J. Fauvre, T. Renno, C. Chaveroux, S.N. Manié, ATF4-Dependent NRF2 transcriptional regulation promotes antioxidant protection during endoplasmic reticulum stress, Cancers 12 (2020) E569, https://doi.org/10.3390/cancers12030569.
[39] Y. Fuse, V.T. Nguyen, M. Kobayashi, Nrf2-dependent protection against acute sodium arsenite toxicity in zebrafish, Toxicol. Appl. Pharmacol. 305 (2016) 136–142, https://doi.org/10.1016/j.taap.2016.06.012.
[40] K. Mukaigasa, T. Tsujita, V.T. Nguyen, L. Li, H. Yagi, Y. Fuse, Y. Nakajima-Takagi, K. Kato, M. Yamamoto, M. Kobayashi, Nrf2 activation attenuates genetic endoplasmic reticulum stress induced by a mutation in the phosphomannomutase 2 gene in zebrafish, Proc. Natl. Acad. Sci. U.S.A. 115 (2018) 2758–2763, https://doi.org/10.1073/pnas.1714056115.
[41] B. Glancy, R.S. Balaban, Role of mitochondrial Ca2+ in the regulation of cellular energetics, Biochemistry 51 (2012) 2959–2973, https://doi.org/10.1021/bi2018909.
[42] R.M. Denton, Regulation of mitochondrial dehydrogenases by calcium ions, Biochim. Biophys. Acta 1787 (2009) 1309–1316, https://doi.org/10.1016/j.bbabio.2009.01.005.
[43] W. Wang, L. Wang, J. Lu, S.L. Siedlak, H. Fujioka, J. Liang, S. Jiang, X. Ma, Z. Jiang, E.L. da Rocha, M. Sheng, H. Choi, P.H. Lerou, H. Li, X. Wang, The inhibition of TDP-43 mitochondrial localization blocks its neuronal toxicity, Nat. Med. 22 (2016) 869–878, https://doi.org/10.1038/nm.4130.
[44] N. Goguadze, E. Zhuravliova, D. Morin, D. Mikeladze, T. Maurice, Sigma-1 receptor agonists induce oxidative stress in mitochondria and enhance complex I activity in physiological condition but protect against pathological oxidative stress, Neurotox. Res. 35 (2019) 1–18, https://doi.org/10.1007/s12640-017-9838-2.
[45] L. de Mena, J. Lopez-Scarim, D.E. Rincon-Limas, TDP-43 and ER stress in neurodegeneration: friends or foes? Front. Mol. Neurosci. 14 (2021), 772226 https://doi.org/10.3389/fnmol.2021.772226.
[46] H. Suzuki, M. Matsuoka, TDP-43 toxicity is mediated by the unfolded protein response-unrelated induction of C/EBP homologous protein expression, J. Neurosci. Res. 90 (2012), https://doi.org/10.1002/jnr.22777.
[47] R. Mutihac, J. Alegre-Abarrategui, D. Gordon, L. Farrimond, M. Yamasaki-Mann, K. Talbot, R. Wade-Martins, TARDBP pathogenic mutations increase cytoplasmic translocation of TDP-43 and cause reduction of endoplasmic reticulum Ca^{2+} signaling in motor neurons, Neurobiol. Dis. 75 (2015) 64–77, https://doi.org/10.1016/j.nbd.2014.12.010.
[48] J. Tong, C. Huang, F. Bi, Q. Wu, B. Huang, H. Zhou, XBP1 depletion precedes ubiquitin aggregation and Golgi fragmentation in TDP-43 transgenic rats, J. Neurochem. 123 (2012) 406–416, https://doi.org/10.1111/jnc.12014.
[49] A.K. Walker, K.Y. Soo, V. Sundaramoorthy, S. Parakh, Y. Ma, M.A. Farg, R. H. Wallace, P.J. Crouch, B.J. Turner, M.K. Horne, J.D. Atkin, ALS-associated TDP-43 induces endoplasmic reticulum stress, which drives cytoplasmic TDP-43 accumulation and stress granule formation, PLoS One 8 (2013), e81170, https://doi.org/10.1371/journal.pone.0081170.
[50] X. Wang, S. Zhou, X. Ding, M. Ma, J. Zhang, Y. Zhou, E. Wu, J. Teng, Activation of ER stress and autophagy induced by TDP-43 A315T as pathogenic mechanism and the corresponding histological changes in skin as potential biomarker for ALS with the mutation, Int. J. Biol. Sci. 11 (2015) 1140–1149, https://doi.org/10.7150/ijbs.12657.
[51] W. Hu, X. Liu, S. Wang, G. Sun, R. Zhao, H. Lu, SecinH3 attenuates TDP-43 p. Q331K-induced neuronal toxicity by suppressing endoplasmic reticulum stress and enhancing autophagic flux, IUBMB Life 71 (2019) 192–199, https://doi.org/10.1002/iub.1951.
[52] S. Oyadomari, M. Mori, Roles of CHOP/GADD153 in endoplasmic reticulum stress, Cell Death Differ. 11 (2004) 381–389, https://doi.org/10.1038/sj.cdd.4401373.
[53] R. Sano, J.C. Reed, ER stress-induced cell death mechanisms, Biochim. Biophys. Acta 1833 (2013) 3460–3470, https://doi.org/10.1016/j.bbamcr.2013.06.028.
[54] L. Crouzier, E.M. Richard, J. Sourbron, L. Lagae, T. Maurice, B. Delprat, Use of zebrafish models to boost research in rare genetic diseases, Int. J. Mol. Sci. 22 (2021) 13356, https://doi.org/10.3390/ijms222413356.
[55] S.R. Barwick, M.S. Siddiq, J. Wang, H. Xiao, B. Marshall, E. Perry, S.B. Smith, Sigma 1 receptor Co-localizes with NRF2 in retinal photoreceptor cells, Antioxidants 10 (2021) 981, https://doi.org/10.3390/antiox10060981.
[56] C.-C. Chou, Y. Zhang, M.E. Umoh, S.W. Vaughan, I. Lorenzini, F. Liu, M. Sayegh, P. G. Donlin-Asp, Y.H. Chen, D.M. Duong, N.T. Seyfried, M.A. Powers, T. Kukar, C. M. Hales, M. Gearing, Nigel J. Cairns, K.B. Boylan, D.W. Dickson, R. Rademakers, Y.-J. Zhang, L. Petrucelli, R. Sattler, D.C. Zarnescu, J.D. Glass, W. Rossoll, TDP-43 pathology disrupts nuclear pore complexes and nucleocytoplasmic transport in ALS/FTD, Nat. Neurosci. 21 (2018) 228–239, https://doi.org/10.1038/s41593-017-0047-3.
[57] K. Pakos-Zebrucka, I. Koryga, K. Mnich, M. Ljujic, A. Samali, A.M. Gorman, The integrated stress response, EMBO Rep. 17 (2016) 1374–1395, https://doi.org/10.15252/embr.201642195.
[58] P.M. Quirós, M.A. Prado, N. Zamboni, D. D'Amico, R.W. Williams, D. Finley, S. P. Gygi, J. Auwerx, Multi-omics analysis identifies ATF4 as a key regulator of the mitochondrial stress response in mammals, J. Cell Biol. 216 (2017) 2027–2045, https://doi.org/10.1083/jcb.201702058.
[59] M.-K. Kwak, N. Wakabayashi, K. Itoh, H. Motohashi, M. Yamamoto, T.W. Kensler, Modulation of gene expression by cancer chemopreventive dithiolethiones through the Keap1-Nrf2 pathway. Identification of novel gene clusters for cell survival, J. Biol. Chem. 278 (2003) 8135–8145, https://doi.org/10.1074/jbc.M211898200.
[60] N. Miyamoto, H. Izumi, R. Miyamoto, H. Bin, H. Kondo, A. Tawara, Y. Sasaguri, K. Kohno, Transcriptional regulation of activating transcription factor 4 under oxidative stress in retinal pigment epithelial ARPE-19/HPV-16 cells, Invest. Ophthalmol. Vis. Sci. 52 (2011) 1226–1234, https://doi.org/10.1167/iovs.10-5775.
[61] C. He, et al., Identification of activating transcription factor 4 (ATF4) as an Nrf2-interacting protein. Implication for heme oxygenase-1 gene regulation, J. Biol. Chem. 276 (2001), https://doi.org/10.1074/jbc.M101198200.
[62] P. Ye, P. Gong, B. Hu, D. Stewart, M. Choi, A. Choi, J. Alam, Nrf2- and ATF4-dependent upregulation of xCT modulates the sensitivity of T24 bladder carcinoma cells to proteasome inhibition, Mol. Cell Biol. 34 (2014) 3421–3434, https://doi.org/10.1128/MCB.00221-14.

Abbreviation

ALS: amyotrophic lateral sclerosis
ATF4: activation transcription factor 4
ATF6: activating transcription factor 6
BiP: Binding immunoglobulin protein
C9orf72: Chromosome 9 open reading frame 72
CHOP: C/EBP homologous protein
DMSO: dimethylsulfoxyde
dpf: day post fertilization
EF1α: ETS-related transciption Factor 1α
EIF2a: Eukaryotic initiation factor 2a
ER: endoplasmic reticulum
FCCP: cyanide-*p*-trifluoromethoxyphenylhydrazone
FTLD: frontrotemporal lobar degeneration
FUS:: Fused in sarcoma

GCLC: Glutamate-cysteine ligase catalytic subunit
GCLM: Glutamate-cysteine ligase modifier subunit
IP3: Inositol triphosphate 3
IRE1: Inositol-requiring enzyme 1
KEAP1: Kelch-like ECH-associated protein 1
NE-100: 4-methoxy-3-*N*,*N*-dipropylbenzeneethanamine
NRF2: Nuclear factor erythroid-2 related factor 2
PERK: Protein kinase RNA-like ER kinase
PGD: Phosphogluconate deshydrogenase
PRDX6: Peroxiredoxin-6
PRE-084: 2-(4-morpholinethyl)-1-phenylcyclohexanecarboxylate hydrochloride
S1R: Sigma-1 receptor
SA4503: 1-(3,4-Dimethoxyphenethyl)-4-(3-phenylpropyl)piperazine dihydrochloride
SOD1: Superoxide dismutase 1
TDP43: Tar-DNA binding protein 43 kDa
UPR: unfolded protein response
VMR: visual motor response
XBP1: X-box binding protein 1
YFP: Yellow fluorescent protein